ORIGINAL PAPER

CrossMark

Properties of Agricultural Films Prepared from Biodegradable Poly(Butylene Succinate) Adding Natural Sorbent and Fertilizer

Nattakarn Hongsriphan[1] 🄳 · Arak Pinpueng[1]

Abstract

Lemon basil (LB) seeds are natural sorbent that would be a good candidate to apply for agricultural application. This study developed a new composite material by compounding biodegradable poly(butylene succinate) (PBS) with grinded LB particles (5, 10, 15 and 20 wt%) and hot pressing into composite films. Ammonium sulfate of 10 phr was loaded as fertilizer. Mechanical and thermal properties as well as moisture sorption and ammonium ion release in water of the composite films were investigated. Composites were characterized by FTIR and SEM. It was found that moisture sorption was enhanced dramatically with respect to LB content. The improved sorption allowed ammonium sulfate to be released faster but reached equilibrium at lower concentration, which the sorption kinetics was fit well following the Pseudo-second order model. Biodegradation of composite films was found to improve in the soil burial test. Nevertheless, adding these fillers caused composite films to be more brittle.

Keywords Agricultural film · Poly(butylene succinate) · Natural sorbent · Moisture sorption · Fertilizer

Introduction

Thailand is well-known to be one of the leading export countries that supply agricultural products to the world to consume directly or to be modified as food or pharmacy. In Thailand, plastic nursery bags made of recycled polyethylene are usually used to grow seedling before transplanting into farms. These bags could be reused until they are torn apart and become plastic waste that could not be recycled. These would lead to many problems [1], for example, these torn bags are discarded, burned or buried on agricultural land. Moreover, the bags discarded on farms can enter waterways and cause blockage leading to flood, and also suffocate aquatic creatures. Muriuki et al. [2] postulated that whether small-scale tree nursery operators were likely to

adopt biodegradable seedling containers (cellulose papers and banana sheaths). They reported that seedlings produced in polyethylene tubes had higher growth rates in the nursery, but when transplanted to the field they were overtaken by those grown in the biodegradable containers due to transplanting shock after the polyethylene containers were removed. Therefore, plastic nursery bags produced from biodegradable polymer films could be one of the feasible solutions that integrate agricultural activities with plastic waste management in Thailand. Several types of biodegradable agricultural films and partially biodegradable films have been researched [3, 4] and produced available commercially [5, 6]. Briassoulis [7] investigated mechanical behavior of thin readily biodegradable starch–polycaprolactone experimental films, which may be used for low tunnels and soil mulching, confirmed that these films showed good mechanical behavior comparable to those of conventional agricultural films (i.e. polyethylene based films).

Poly(butylene succinate) (PBS) is an interesting biodegradable polymer with a range of suitable properties including biodegradability [8], melt processability, and moderate mechanical properties comparable to polyethylene. The commercial applications of PBS are mainly implemented in packaging fields, such as food and cosmetic packaging; disposable products such as medical articles, and in

✉ Nattakarn Hongsriphan
  Hongsriphan_N@su.ac.th

[1] Department of Materials Science and Engineering, Faculty of Engineering and Industrial Technology, Silpakorn University, Sanamchandra Palace Campus, Nakhon Pathom 73000, Thailand

agricultures, such as mulching films. Nevertheless, PBS is relatively high cost and has low water sorption. In the previous work, Sriakkarakul and Hongsriphan [9] prepared thin sheets of PBS and superabsorbent polymer (SAP) blends loaded with ammonium sulfate ($(NH_4)_2SO_4$) as a source of fertilizer for plant growth. The commercial SAP was based on poly (acrylicacid-co-acrylamide) [10] that had particle sizes of 200–1000 µm. The blend performance was evaluated in terms of moisture sorption and ammonium ion release in water. It was found that the excellent moisture sorption performance of PBS/SAP blend was attributed to the chemical hydrophilic groups and network structure in SAP. Also, the presence of SAP clearly benefitted for ammonium ion (NH^{4+}) release in the blend sheets due to the combination of fast moisture sorption by SAP and easier access of water molecules through opening gaps at the interface between PBS and SAP. Unfortunately, producing such a blend for practical use would be discouraged due to cost add-up.

Lemon basil (*Ocimun basilicum* L.) is a popular culinary herb grown in many parts of the world [11] that it is used for flavoring food, in cosmetics and in traditional medicine for the treatment of respiratory and urinary tracts inflammation [12], cough or asthma [13]. In Thailand, Lemon basil seeds (locally called maeng lak) are used to produce traditional dessert. The unique characteristics of basil seeds is that they adsorb water very well forming translucent gel-like membrane around the seeds serving as a natural source of exopolysaccharides. Shamsnejati et al. [14] studied the use of basil seeds as an active natural coagulant and reported that these seeds provided highly effective coagulant agent for the treatment of textile wastewater, which only 1.6 mg/L of the coagulant had the ability to decolorize congo red dye solution with a concentration of 250 mg/L. Khazaei et al. [15] developed edible films from basil seed gum (BSG) and glycerol as plasticizer with three different concentrations (25%, 35%, and 50% w/w). They reported that the prepared films were transparent with good mechanical properties and excellent barrier properties. At the level of 25% w/w of glycerol, BSG films had the lowest water vapor permeability values and the highest values for tensile strength.

Since Lemon basil seeds in Thailand is inexpensive and abundant in the market, they are interested to produce biodegradable polymeric material. In this study, a new biodegradable film was developed by melt blending PBS with grinded Lemon basil seeds in the weight ratio of 100/0, 95/5, 90/10, 85/15, and 80/20 wt%. Ammonium sulfate ($(NH_4)_2SO_4$) of a fixed content (10 phr) was also incorporated as fertilizer. Lemon basil seeds did not only serve as natural moisture sorbent for the blend but also reduced cost of the prepared composite films. Fourier-transform infrared (FT-IR) spectroscopy was used to characterize their functional groups. Tensile properties of hot pressed composite films were evaluated and compared with PBS films, which morphology of

fracture surface was studied by scanning electron microscopy. Moisture sorption and ammonium ion release in water were investigated and compared with unloaded PBS film. Finally, soil burial test was carried out to investigate influence of these fillers on biodegradation of the developed composite films.

Experimental

Materials

PBS (GS Pla®, FZ91PD) with MFI of 6 g/10 min (190 °C, 21.18 N) was purchased from Mitsubishi Chemicals, Japan. Lemon basil seeds (black seeds with diameter of about 1 mm) were purchased from Thai Cerals World Co., Ltd., Thailand. Other chemicals were ammonium sulfate ($(NH_4)_2SO_4$) (Ajax Finechem Pty. Ltd.), Sodium nitroprusside dihydrate ($Na_2[Fe(CN)_5NO]\cdot2H_2O$) (Fluka), Sodium citrate ($HOC(COONa)$ $(CH_2COONa)_2\cdot2H_2O$) (Omega chemical corp.), Phenol crystallized (C_6H_5OH) (QRëC), Sodium chloride (NaCl), Sodium hydroxide (NaOH) (ACI lab scan Ltd.), ethanol 95%, and deionized water. All chemicals were analytical grade and used as received.

Composite Preparation and Fabrication

Reduction of Particle Sizes

Dried Lemon basil seeds were grinded using a high speed mixer for 10 min, then dried in an air-circulating oven at 60 °C for 3 h to evaporate essential oil, and grinded again for another 10 min. Then, grinded particles were sieved to obtain particle sizes less than 300 µm. As-received ammonium sulfate particles were ball milled and sieved to obtain particle sizes < 150 µm.

Melt Compounding and Film Fabrication

Prior to melt compounding, PBS pellets, sieved Lemon basil particles (LB), and sieved ammonium sulfate were dried in an air-circulating oven at 60 °C for 12 h. The mass ratios of PBS/LB were varied from 100:0, 95:5, 90:10, 85:15, and 80:20 wt%, which ammonium sulfate was added at a fixed content of 10 phr in each blend composition. Table 1 presents the compositions and their abbreviations.

Each composition was melt blended using a co-rotating twin-screw extruder (SHJ-25, S/D 40, Yongteng, China) with a screw speed of 60 rpm which the barrel temperature was set at 140–170 °C. The extrudates were air cooled at ambient temperature in order to prevent water absorption during the melt compounding, then pelletized and kept in a sealed plastic bags filled with silica gel beads in order to

Table 1 Composition and abbreviations of neat PBS and composite films

Abbreviation	PBS (wt%)	Lemon basil particles (wt%)	Ammonium sulfate (phr)
PBS	100	0	–
PBS_L5	95	5	–
PBS_L10	90	10	–
PBS_L15	85	15	–
PBS_L20	80	20	–
PBS_N	100	0	10
PBS_LN5	95	5	10
PBS_LN10	90	10	10
PBS_LN15	85	15	10
PBS_LN20	80	20	10

prevent moisture pickup. Sample films (200 ± 5 μm thickness) were fabricated using a hot pressing machine (LP-S-50, Labtech Engineering Co. Ltd., Thailand) at temperature of 160 °C and pressing pressure of 120 bar. Sample films were kept in polyethylene bags filled with silica gel beads.

Characterization and Testing

Fourier Transforms Infrared Spectroscopy (FTIR) Analysis

Samples were dried in an air-circulating oven for 24 h, grinded and mixed with dried KBr powder, and hydraulic pressed into KBr discs. They were studied using a Fourier transform infrared (FT-IR) spectrometer (Vertex 70, Bruker, Germany) in the range 4000–400 cm^{-1}. Spectra were obtained using 32 scanning and a resolution of 4 cm^{-1}.

Tensile Test

Sheet samples were cut into rectangular strips (2.54×15.24 cm^2) for tensile test using a universal testing machine (Instron model 5969, Instron Engineering Corporation, USA). The tests were carried out in accordance to ASTM-D882 using a constant strain rate of 5.0 mm/min. The gauge length was set at 10.16 cm. Modulus, tensile strength, and elongation at break were obtained from the tests. Fifteen samples were tested for each composition, which the average and standard deviations were calculated and reported.

Morphology by Scanning Electron Microscopy (SEM)

Cross-sectional fracture surface of sample films were studied using a scanning electron microscope (Tabletop Microscope TM3030, Hitachi, Japan). Prior to studying, sample surfaces

were sputtering coated with platinum in order to avoid electrostatic charging.

Thermal Properties by Differential Scanning Calorimeter (DSC)

Sample films were cut into small pieces (5–10 mg) for thermal properties analysis using a differential scanning calorimeter (DSC1, Mettler Toledo, USA). The tests were performed in heat-cool-reheat mode from 20 to 150 °C with a heating/cooling rate of 10°C/min under nitrogen atmosphere. Melting temperature and crystallization temperature were determined from the thermograms. The degree of crystallinity (X_c) was calculated from the second heating thermogram by the following equation.

$$X_c = \frac{\Delta H_m}{\Delta H_m^o X_{PBS}} \times 100 \qquad (1)$$

where ΔH_m was the melting enthalpy of the composite, X_{PBS} was the PBS weight fraction in the composite, and ΔH_m^o was the melting enthalpy for a 100% crystalline PBS polymer, which was equal to 110.3 J/g [16].

Moisture Sorption Measurement

Sample films were cut into 60×30 mm^2 (200 ± 5 μm thickness), and dried in an air-circulating oven at 50 ± 2 °C for 8 h (this weight was designated w_c). Thereafter, the samples were put in a desiccator containing sodium chloride (NaCl) solution that gave 75%RH at room temperature (≈ 30 °C). The percentage of weight increased due to humidity sorption (w_f) was calculated the following Eq. (1) [16]:

$$\%w_f = \frac{W_w - W_d}{W_d} \times 100\% \qquad (2)$$

where w_w was the sample weight at various intervals and w_d was the dried sample weight. All raw data generated in the study are included in the supplementary material.

Release of Ammonium Ions in Deionized Water

Sample films were cut into 60×30 mm^2 (200 ± 5 μm thickness) and placed in beakers containing 500 ml deionized water (release medium) without stirring and allowed ammonium sulfate to release at ambient temperature (≈ 30 °C). At various intervals, 2 ml solutions were drawn from the medium to follow the release of ammonium ions (NH^{4+}). The released ions were determined by a spectrophotometric method following the ammonia determination method (modified from Parsons et al. 1984) with a UV–Vis spectrophotometer (v530, Jasco) to determine maximum absorbance in the wavelength range of 640 nm with scanning rate of

200 nm/min. All raw data generated in the study are included in the supplementary material.

Soil Burial Test

Conditioned soils were prepared by mixing natural soil of 20 kg with bacterial powder of 80 g and water of 10 l. The mixing ingredients were covered with black plastic films under monitored moisture of $90 \pm 5\%$ (watering) for 7 days to allow growth of bacteria. Sample films were cut to be 16×16 cm^2 (200 ± 5 μm thickness) and dried in a vacuum oven for 24 h. The sample films was buried under conditioned soils at 10 cm depth. At 30, 60, and 90 days, the sample films were withdrawn from conditioned soils to take photo.

Results and Discussion

FT-IR Measurements

In order to study chemical compatibility among phases in the samples, FTIR was used to evaluate spectrum shifting of the main functional groups. Figure 1 shows FTIR spectra of PBS, PBS_N, PBS_L20 and PBS_LN20 samples. In Fig. 1a, the spectra of PBS shows characteristic ester peaks at 1700 cm^{-1} for the stretching vibration of the –C=O carbonyl and at 1326 cm^{-1} for the stretching vibration of the C–O– carbonyl [17]. The broad spectrum between 3400 and 3600 cm^{-1} is assigned as –O–H stretching from –COOH in chain ends of PBS. In Fig. 1b, the spectra of PBS_N sample shows at 3140 cm^{-1} attributed to NH_4^+ asymmetric stretching, at 1463 cm^{-1} attributed to NH_4^+ deformation and at 1110 cm^{-1} attributed to SO_4^{2-} stretching of ammonium

Fig. 1 FT-IR spectra of (a) PBS, (b) PBS_N, (c) PBS_L20 and (d) PBS_LN20

sulfate [18]. From FTIR spectrum, the interaction between ammonium sulfate and PBS is not clearly indicated. In Fig. 1c, the presence of LB particles in PBS matrix shifts the spectrum of hydroxyl group slightly from 3432 to 3431 cm^{-1} indicating the H-banding between phases. The sharp spectrum at 1400 cm^{-1} is assigned to C–OO symmetric stretching, which Gahruie et al. [19] assigned as the presence of uronic acid in basil seeds.

The broad spectrum at 3132 cm^{-1} is assigned to the hydroxyl groups from this acid. In Fig. 1d, the spectra is mostly similar to that of Fig. 1c, however, the spectrum at 1121 cm^{-1} assigned for SO_4^{2-} stretching is somewhat broaden implying weaker interaction of NH_4^+ inside ammonium sulfate particles. This shifting indicates that there is chemical interaction between the hydroxyl groups (polysaccharide) of LB particles and ammonium sulfate particle. Shamsnejati et al. [14] observed the shifting of basil gum's spectrum after absorbed dye and suggested that there was particle–polymer–particle complex formation where the polysaccharides served as a bridge.

Tensile Properties of PBS and Composite Films

In order to be applied as nursery bags, tensile properties of the developed composite films had to be evaluated how tough they were after adding these fillers. Figure 2 shows tensile modulus, tensile strength at break, and elongation at break of the composite films compared with PBS films.

Obviously, adding ammonium sulfate of 10 phr increased tensile modulus but reduced tensile strength and elongation at break of the composite films. Aggregated ammonium sulfate restricted mobility of PBS molecules so that they reinforced the PBS matrix for rigidity. On the other hand, this constraint caused tensile strength reduced from 27.38 MPa to 22.84 MPa (16.58% loss) and elongation at break to be reduced in half compared to the original value. This was related to the weak interfacial adhesion between the hydrophilic ammonium sulfate particles and the hydrophobic PBS matrix, similarly to the study by Lee et al. [16] that compounded PBS with kenaf fibers of 30 wt%.

Adding LB particles increased rigidity of the composite films, which the maximum tensile modulus was obtained when LB particles of 10 wt% and ammonium sulfate of 10 phr. It is well known that mechanical properties of fiber-reinforced composites depend on aspect ratio of the fibers. Kwon et al. [20] compounded PLA with kenaf fibers and corn husk flour at which the aspect ratio of kenaf fiber was higher than that of corn husk flour. They found that the tensile modulus of composites were increased when the amount of kenaf fiber compared to corn husk flour was largely incorporated in composites. In this study, Lemon basil seeds were high-speed cut into particle size less than 300 μm. These basil particles were
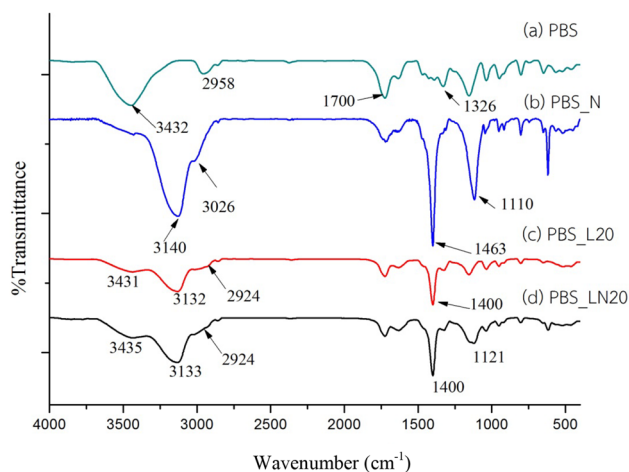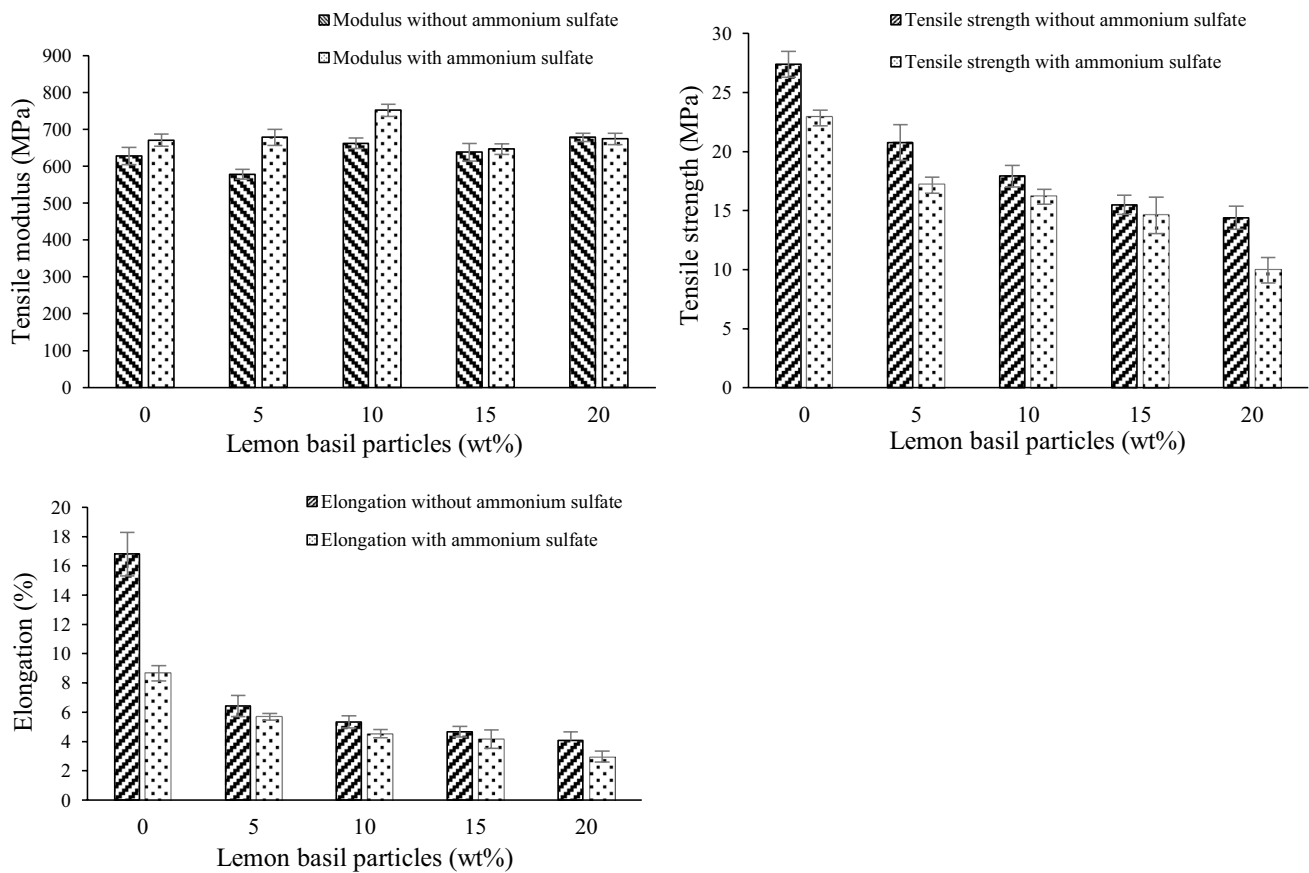
Fig. 2 Tensile modulus, tensile strength at break, and elongation at break of PBS, PBS_N, and PBS_LN sample films

more like particulate fillers than reinforcing fibers, so that the stress transfer from the matrix to the fillers is insufficient to enhance the material fracture strength [16].

In terms of film toughness, tensile strength and elongation at break of the composite films were analyzed. It was found that tensile strength and elongation at break of the composite films decreased significantly with higher filler contents implying toughness of PBS was deteriorated after adding fillers. Decreasing of tensile strength was due to poor stress transfer between PBS matrix and fillers. Although the possible interaction between PBS matrix and these fillers was observed in FTIR spectra, the stress transfer would be hindered by filler shapes and aggregation so that these fillers acted like stress concentrators in the polymeric matrix. The fracture would be initiated at the interface and propagated through the matrix, which correlated with the SEM micrographs showing brittle fracture behaviour. From the mechanical results, it indicated that the composite films should have a suitable thickness to withstand applied stress during the planting.

Morphology by SEM

Figure 3 presents SEM micrographs of cross-sectional fracture surfaces from PBS film and composite films in the study. Clearly, ammonium sulfate particles were not miscible with PBS matrix in the PBS_N sample although the particles were evenly distributed. This was in contrast to adding calcium carbonate particle into PBS matrix that homogeneous dispersion was reported [21, 22]. Aggregates were observed due to fast moisture pickup of ammonium sulfate during the compounding. For PBS_L sample, Lemon basil particles separated from the PBS matrix which small voids were observed around the matrix. The same observation was found by Liminana et al. [23] that uncompatibilized composites between PBS and Almond shell flour (ASF) showed poor particle-polymer interaction which there were voids between ASF particles and the surrounding PBS matrix. Compared to PBS film, all PBS_N and the PBS_LN composite films failed in brittle behaviour showing rougher surfaces with emerging fillers.
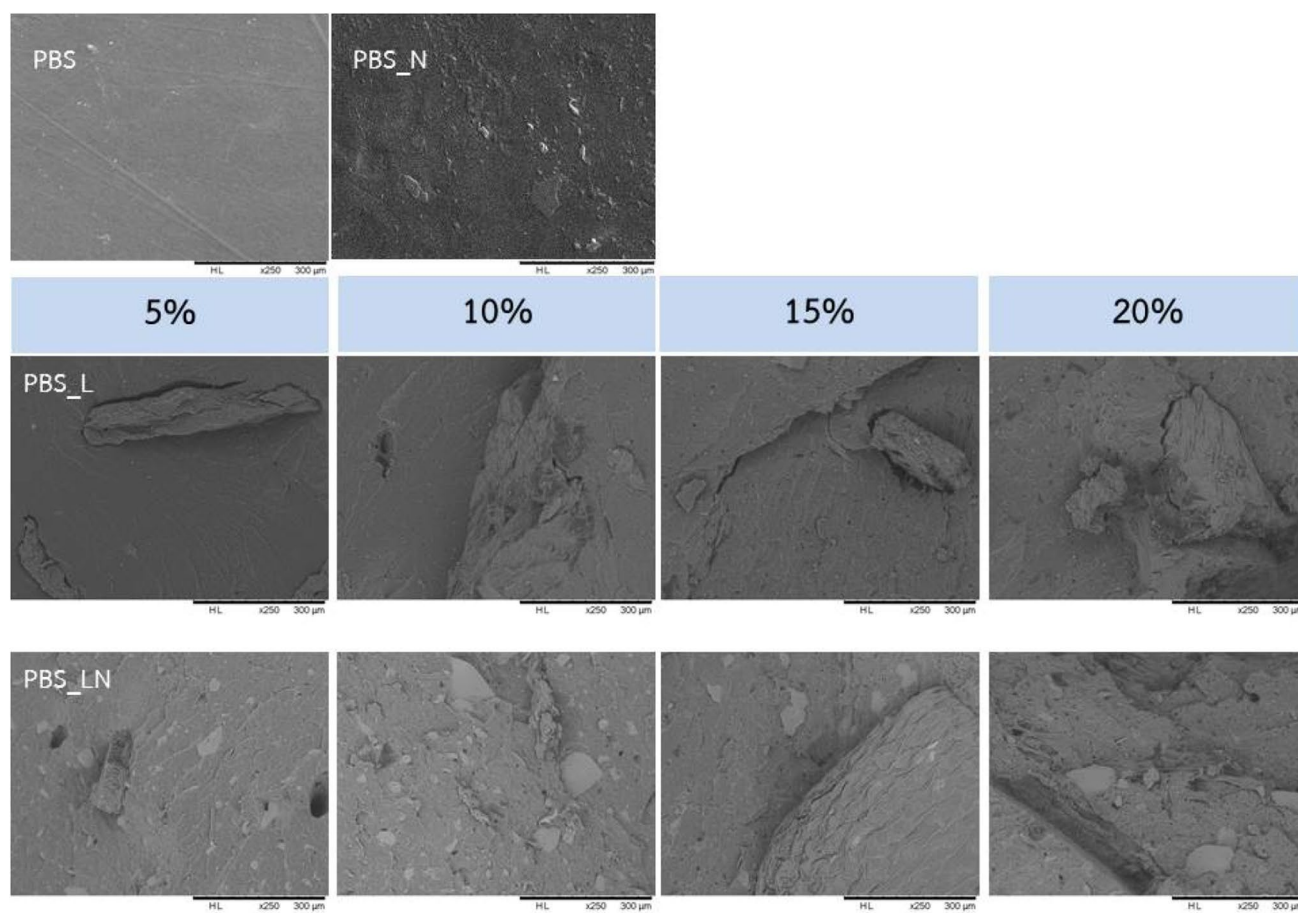
Fig. 3 SEM micrographs of cross-sectional samples from PBS, PBS_N, PBS_L and PBS_LN films (magnification of ×250)

Thermal Properties by DSC

Since PBS is semi-crystalline polymer, degree of crystallinity is important for various properties, such as mechanical property, water sorption, and biodegradability. Thermal properties of PBS film and composite films were thus studied using DSC technique. Figure 4 presents the 2nd heating and the cooling DSC thermogram of PBS, PBS_N, PBS_L, and PBS_LN samples, which Table 2 summerizes melting temperatures, cooling temperatures, and degree of crystallinity of these samples.

It is seen that both ammonium sulfate and Lemon basil particles acted as nucleating agents in the PBS crystallization, which they increased the onset crystallinity temperature from 77 °C to about 90 °C. As a result of promptly nucleation, the degree of crystallinity of all composites were increased significantly compared to PBS sample. The melting temperatures showed similar pattern with slightly shift of values implying the crystal structures were not altered by the fillers. It was found that adding Lemon basil particles of 10 wt% gave the maximum degree of crystallinity whether ammonium sulfate was added or not.

Moisture Sorption of PBS and Composite Films

Hydrophilic groups and degree of crystallinity play important role in moisture sorption of composite films. In this work, material is aimed to be used in agricultural application, thus the sorption for retention water in soil is needed to achieve as other report did [24]. Figure 5 shows moisture sorption of composite films compared with PBS film. It is seen that the content of Lemon basil (LB) particles had high impact on moisture sorption of these developed composite films. Adding 20 wt% LB particles into PBS increased moisture absorbency from 0.65 to 2.53 wt% (289% increase). This confirmed the role of the hydrophilic groups (cellulose and/or hemicelluloses) of LB particles that were able to adsorb moisture to form gelatinous substance in the composite films. In addition, water molecules could diffuse and encapsulated in the voids at interphase of PBS and LB particles.

In Fig. 5, comparison between PBS and PBS_N, it was found that adding ammonium sulfate into PBS matrix decreased moisture sorption to be less than pure PBS. This correlates with the increase of degree of crystallinity in the
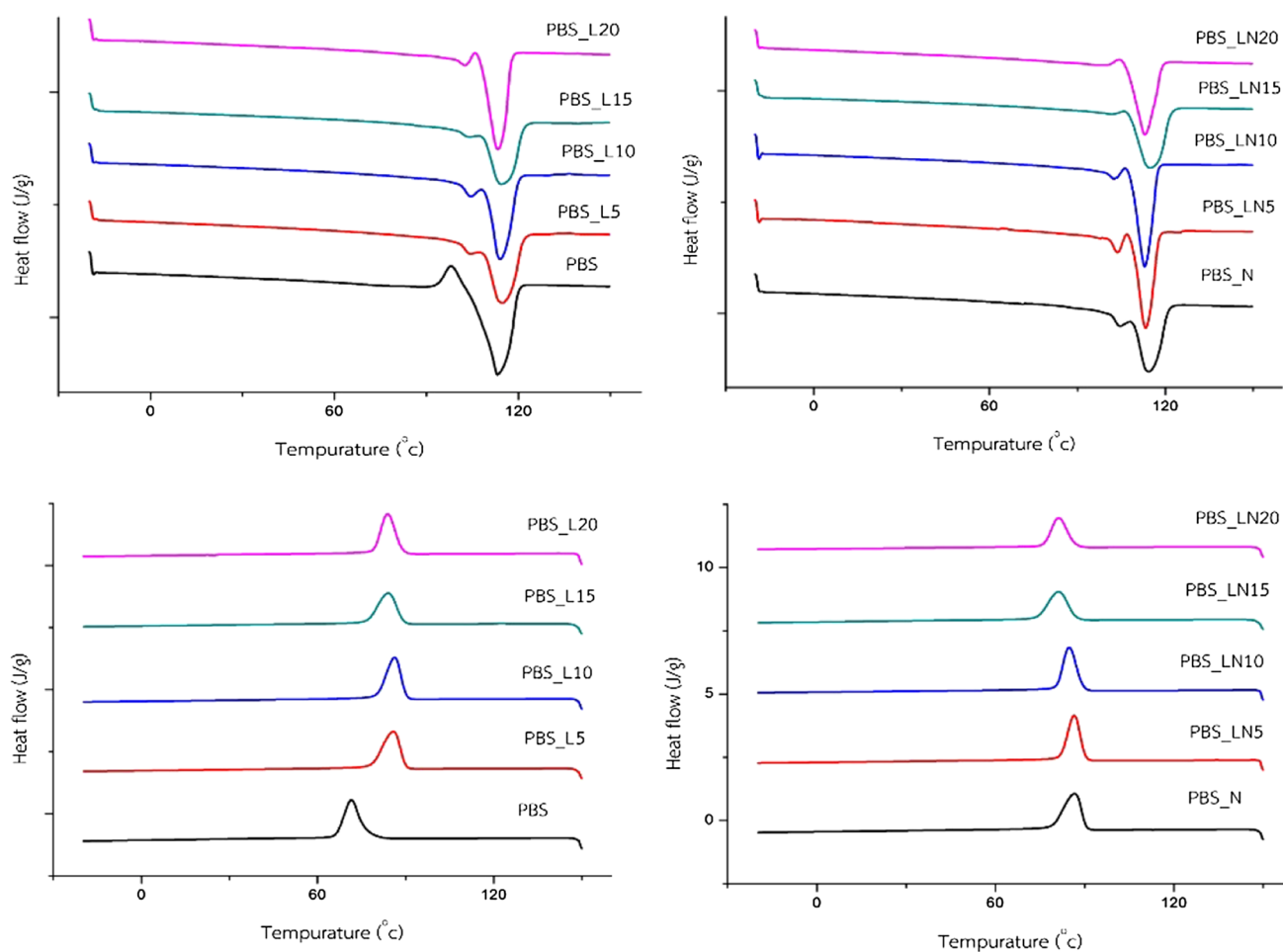
Fig. 4 DSC thermogram (2nd heating and cooling) of PBS, PBS_L, PBS_N and PBS_LN

Table 2 Melting temperatures (T_m), crystallization temperatures (T_c), and degree of crystallinity (%X_c) of PBS, PBS_N, PBS_L and PBS_LN samples

| Samples	Cooling step		2nd Heating step		
	$T_{c,onset}$	$T_{c,peak}$	$T_{m,onset}$	$T_{m,peak}$	%X_c
PBS	76.80	66.35	106.35	119.90	53.58
PBS_N	90.54	79.23	99.64	120.99	66.61
PBS_L5	89.98	78.52	98.56	121.59	69.86
PBS_L10	90.23	80.36	99.00	120.02	74.79
PBS_L15	89.24	77.07	96.43	121.63	69.08
PBS_L20	88.79	79.30	96.82	117.69	69.53
PBS_LN5	90.23	81.98	99.79	117.91	64.40
PBS_LN10	89.43	80.74	96.94	117.48	72.49
PBS_LN15	86.99	74.26	86.61	121.75	70.59
PBS_LN20	86.74	76.42	76.28	118.93	63.22
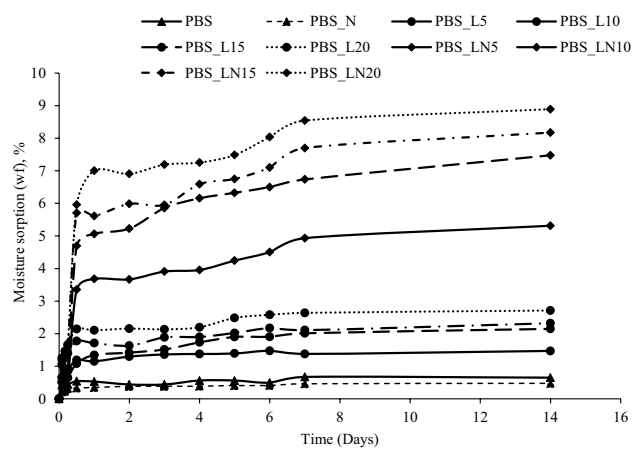
Fig. 5 Moisture sorption of PBS, PBS_L, and PBS_LN composite films

PBS_N film as evident in DSC result. Also, there might have less active sites for water sorption at the surface due to the interaction between NH_4^+ ions and hydroxyl groups at the chain ends of PBS [9]. When adding both LB particles and ammonium sulfate, the moisture sorption jumped to much higher values and still increased with respect to LB contents. For example, the moisture content (w_f) in PBS_LN20 sample was increased from 0.65 to 8.89% (1267% increase). This would be attributed to the initial sorption of H_2O molecules introduced by hydroxyl groups in LB particles, and then transferred to the surrounding ammonium sulfate that was highly hydrophilic (water soluble).

In order to study sorption kinetic of moisture sorption, these data were treated in the Pseudo-second order (PSO) model which the equation could be shown as the following [25].

$$\frac{dq_t}{dt} = k_2 \left(w_\infty - w \right)^2 \tag{3}$$

when w was sorption content at any time (g), w∞ was weight of sorption at equilibrium state (g), t was sorption time (day), and k2 was rate constant of sorption (per g day).

When equation was integrated at $t=0$–t and $q_t=0$–q_t, the linear equation would be obtained as shown in the following equation.

$$\frac{t}{w} = \frac{1}{k_2 w_\infty^2} + \frac{1}{w_\infty} t \tag{4}$$

Thus, a plot of t/w against t of Eq. (4) should give a linear relationship with a slope of $1/w_\infty$ and an intercept of $1/k_2 w_\infty^2$.

Also, the initial sorption (h) could be calculated by the following equation.

$$h = k_2 \left(w_\infty \right)^2 \tag{5}$$

when h was the initial sorption rate (g/day).

And, half time for sorption until reaching equilibrium can be calculated by the following equation.

$$t_{1/2} = \frac{1}{k_2 w_\infty} \tag{6}$$

when $t_{1/2}$ was half time of sorption (day).

Figure 6 shows the Pseudo-second order fitting curves and Table 3 summarizes the Pseudo-second-order rate parameters for moisture sorption into sample films. It is seen that the coefficient of determination (R^2) was 0.97–0.99

Table 3 Pseudo-second-order rate parameters for moisture sorption into sample films

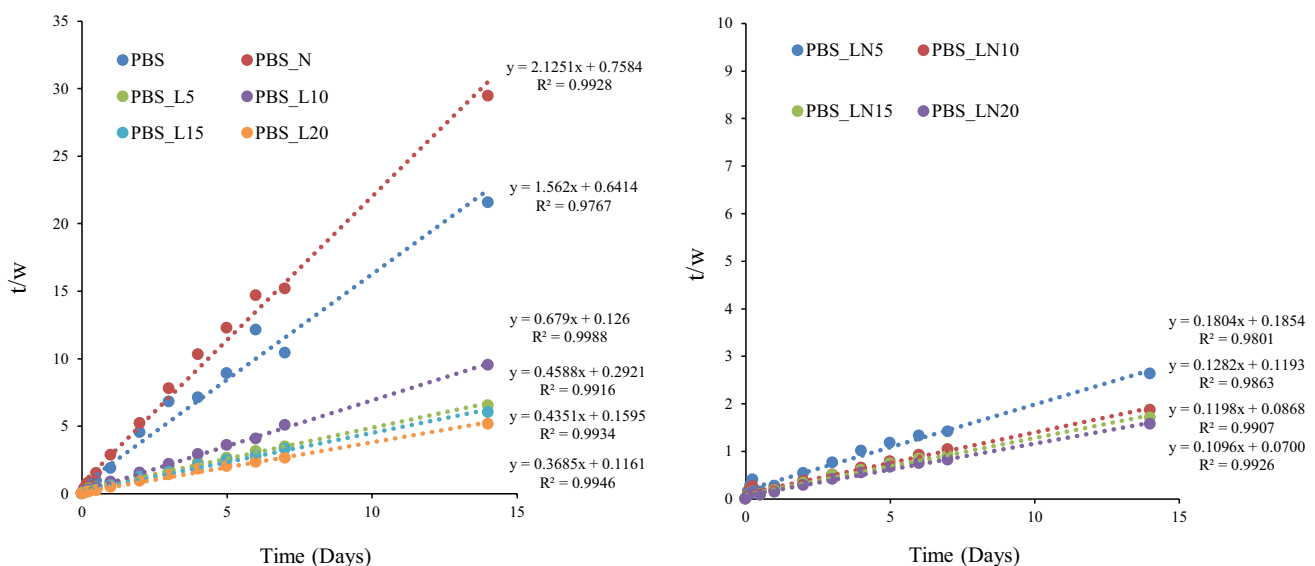| Sample	k_2	R^2	h (g/day)	$t_{1/2}$ (day)
PBS	2.433	0.9767	0.996	0.6423
PBS_N	2.797	0.9928	0.620	0.7591
PBS_L5	1.572	0.9916	7.463	0.2920
PBS_L10	5.380	0.9988	11.672	0.1262
PBS_L15	2.726	0.9934	14.401	0.1596
PBS_L20	3.169	0.9946	23.334	0.1163
PBS_LN5	0.973	0.9801	29.883	0.1855
PBS_LN10	1.073	0.9863	65.275	0.1195
PBS_LN15	1.377	0.9907	96.136	0.0869
PBS_LN20	1.566	0.9926	130.344	0.0700

Fig. 6 The Pseudo-second order fitting curves

indicating that the moisture sorption data was very good fitting with the applied equation. From the fitting model, this points that the kinetics of moisture sorption into PBS and PBS-based composite films was chemical sorption which involved valency forces through sharing or exchange of electrons between the sorbent (LB particles) and the sorbate (water molecules) [26].

Considering the rate constants, it indicates that the adding ammonium sulfate into PBS reduced the initial sorption rate and increased half time of sorption (or time to reach sorption equilibrium), however, the sorption rate was slightly higher. This correlated to the interaction between PBS matrix and ammonium sulfate that reduced the ability to attract water molecules. In contrast, adding LB particles increased the initial sorption rate dramatically and reduced half time of sorption from 0.6423 days (about 15 h) to be 0.1163–0.2920 days (2.8–7.0 h). When adding both LB and ammonium sulfate, the initial sorption rate was further enhanced which the half time of sorption was between 0.070 days (1.7 h) and 0.1855 days (4.4 h). The enhancement of moisture sorption by LB particles would be benefit for seedling since the composite film could adsorb moisture very well during watering.

Release of Ammonium Ions in Water

Figure 7 shows ammonium ion concentration released from PBS and composite films. In this work, the concentration of ammonium sulfate $((NH_4)_2SO_4)$ was fixed constant at 10 phr. Since ammonium sulfate was mixed directly into hydrophobic PBS matrix, the rate of nitrogen ion release in the ammonium ion form (NH_4^+) depended on how much and how fast water molecules could diffuse into the PBS matrix in order to dissolve $(NH_4)_2SO_4$ salts and to release NH_4^+ ions into deionized water. It was found that the NH_4^+ ion was released faster when adding LB particles more than 5 wt%. Water sorption was induced better by these LB particles so
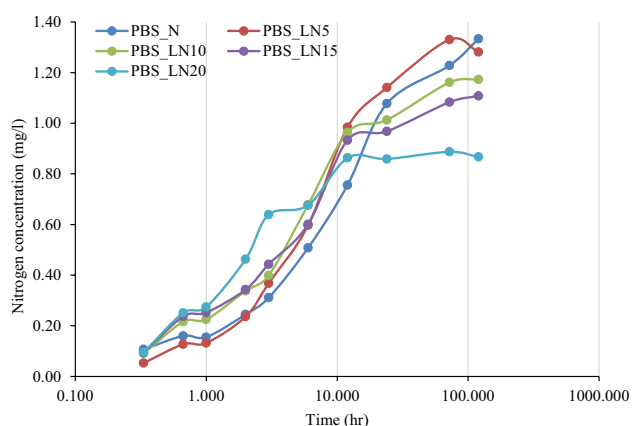
that ammonium sulfate was dissolved and released from the film samples into water. However, after 10 h the rate of NH_4^+ ion release was slower in these composite films, except the PBS_N and PBS_LB 5 wt% showed steadier rate of NH_4^+ ion release. This behaviour resulted from LB particles became gelatinous substance in the film samples that inhibited desorption of NH_4^+ ions from the films. PBS_LN20 reached the equilibrium of NH_4^+ ion release after 24 h, while PBS_LN10 and PBS_LN15 reached the equilibrium of NH_4^+ ion release after 72 h. From the finding, it suggested that PBS_LN10 was the best composition since it provided faster rate of NH_4^+ ion release than PBS_N, and it still released NH_4^+ ions in considerable high concentration after 24 h.

Soil Burial Test

Figure 8 shows photo images of PBS, PBS_N, PBS_L10, PBS_L20, PBS_LN10, and PBS_LN20 films after being burial in conditioned soils for various times. It should be noted that the soil burial test in this study was not the standard biodegradation test, only conducted to compare the biodegradability of the prepared samples under the control condition. The biodegradation in natural environment would occur at different biodegradation rate. It is seen that adding LB particles helped acceleration of biodegradation of PBS matrix. This was due to LB particles could absorb moisture and also microorganism from conditioned soils better than neat PBS film, which microorganism digested carbohydrates
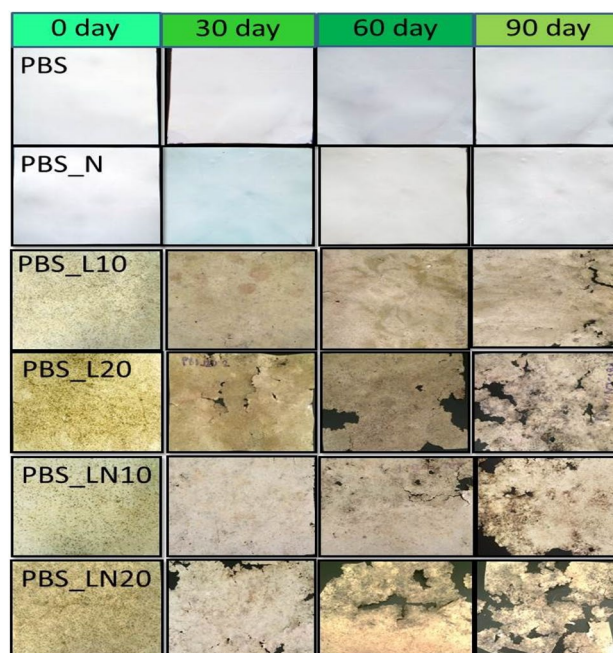

Fig. 7 Effect of ammonium sulfate and Lemon basil particle content on nitrogen ion release from composite films

Fig. 8 Photo of PBS and composite films showing biodegradation in soil

in LB particles and then PBS matrix as well. Adding ammonium sulfate into composite films showed higher loss of film matter during the soil burial. This came from the fact that ammonium sulfate could dissolve by adsorbed water and diffuse into surrounding soil. Also, the faster rate of moisture sorption in these PBS_LN composite films would allow higher concentration of microorganism to go through the composite mass for the biodegradation mechanism. This finding was similar to that reported by Huang et al. [27] that the introduction of sugarcane rind fiber (SRF) could accelerate the degradation of PBS matrix. They suggested that the hydrophilic group of SRF absorbed more water and microorganisms causing a significant number of pores and grooves appeared on the composite surface after soil burial.

Conclusion

Grinded Lemon basil (LB) particles was successfully melt blended with PBS along with a fixed content of ammonium sulfate as fertilizer and then the compounding was hot pressed into composite films. From SEM micrographs, it showed that LB particles and ammonium sulfate particles were not miscible and distributed in PBS matrix with some voids were observed around the particles. FITR spectra indicated there were interaction between the hydroxyl groups (polysaccharide) of LB particles and ammonium sulfate particle. These fillers acted as nucleating agents to increase degree of crystallinity of PBS and reinforced to improve rigidity of the composite films. However, toughness of composite films were reduced because these fillers became stress concentrators. Increasing LB contents increased moisture sorption of the composite films, which allowed ammonium sulfate to be released faster but reached equilibrium at lower concentration. The sorption kinetics was fit well following the Pseudo-second order model, which sorption parameters were calculated to demonstrate and compare. From soil burial test, it was shown that biodegradation of composite films was accelerated from the presence of these fillers.

References

1. Ouya D (2013) Biodegradable seedling bags could grow stronger trees, but can they replace polythene? Agroforestry World. http://blog.worldagroforestry.org/index.php/2013/08/20/biodegradable-seedling-bags-could-grow-stronger-trees-but-can-they-replace-polythene/. Cited 2018 April 17
2. Muriuki JK, Kuria AW, Muthuri CW, Mukuralinda A, Simons AJ, Jamnadass RH (2014) Small-scale For 13:127–142
3. Finkenstadt VL, Tisserat B (2010) Ind Crops Prod 31:316–320
4. Ma Z, Ma Y, Qin L, Liu J, Su H (2016) Int Biodeterior Biodegrad 111:54–61
5. Touchaleaume F, Martin-Closas L, Angellier-Coussy H, Chevillard A, Cesar G, Gontard N, Gastaldi E (2016) Chemosphere 144:433–439
6. Briassoulis D, Giannoulis A (2018) Polym Test 67:99–109
7. Briassoulis D (2004) J Polym Environ 12:65–81
8. Pan W, Bai Z, Su T, Wang Z (2018) Int J Biol Macromol 111:1040–1046
9. Sriakkarakul M, Hongsriphan N (2012), Moisture absorption and fertilizer release of poly(butylene succinate) blended with fertilizer loaded superabsorbent polymer for using in agriculture application. In: The 10th Eco-Energy and Materials Science and Engineering Symposium, Ubon Rachathani
10. Yang J, Gao J, Wang X, Mei S, Zhao R, Hao C, Wu Y, Zhai X, Liu Y (2017) J Nanoparticle Res 19:350–363
11. Varga F, Carović-Stanko K, Ristić M, Grdiša M, Liber Z, Šatovi Z (2017) Ind Crops Prod 109:611–618
12. Raina P, Agarwal DM,CCV,A, Wagh N, Kaul-Ghanekara R (2016) J Herb Med 6:28–36
13. Arranz E, Jaime L, LópezdelasHazas MC, Reglero G, Santoyo S (2015) Ind Crops Prod 67:121–129
14. Shamsnejati S, Chaibakhsh N, Pendashteh AR, Hayeripour S (2015) Ind Crops Prod 69:40–47
15. Khazaei N, Esmaiili M, Djomeh ZE, Ghasemlou M, Jouki M (2014) Carbohydr Polym 102:199–206
16. Lee JM, Ishak ZAM, Taib RM, Law TT, Thirmizir MZA (2013) J Polym Environ 21:293–302
17. Siracusa V, Lotti N, Munari A, Rosa M (2015) Polym Degrad Stab 119:35–45
18. Boer GJ, Sokolik IN, Martin ST (2007) JQSRT 108:17–38
19. Gahruie HH, Ziaee E, Eskandari MH, Hosseini SMH (2017) Carbohydr Polym 166:93–103
20. Kwon H-J, Sunthornvarabhas J, Park J-W, Lee J-H, Kima H-J, Piyachomkwa K, Sriroth K, Choe D (2014) Composite B 56:232–237
21. Bosq N, Aht-Ong D (2018) JTAC 132:233–249
22. Hongsriphan N, Burirat T, Niratsungnern P, Trongteng S (2013) JMMM 23:41–47
23. Liminana P, Garcia-Sanoguera D, Quiles-Carrillo L, Balart R, Montanes N (2018) Composite B 144:153–162
24. Liang R, Yuan H, Xi G, Zhou Q (2009) Carbohydr Polym 77:181–187
25. Hoa Y-S, Ofomaja AE (2006) J Hazard Mater 129:137–142
26. Okewale AO, Babayemi KA, Olalekan AP (2013) IJASET 3:35–42
27. Huang Z, Qian L, Yin Q, Yu N, Liu T, Tian D (2018) Polym Test 66:319–326